JOURNAL OF GEOPHYSICAL RESEARCH, VOL. 103, NO. A3, PAGES 4145–4155, MARCH 1, 1998

Ion cyclotron waves during a great magnetic storm observed by Freja double-probe electric field instrument

T. Bräysy and K. Mursula

Department of Physical Sciences, University of Oulu, Oulu, Finland

G. Marklund

Royal Institute of Technology, Alfvén Laboratory, Stockholm, Sweden

Abstract. Evolution of the great magnetic storm in April 1993 is studied using observations of electromagnetic ion cyclotron (EMIC) waves by the F1 double-probe electric field instrument onboard the Freja satellite. The almost continuous operation of the F1 instrument in the overview mode allowed us to follow the global EMIC wave activity at low altitudes above the ionosphere during several subsequent days covering the initial (compression), main, and recovery phases of the storm. During the initial phase of the storm the spatial occurrence of EMIC waves has a postnoon high-latitude maximum, in agreement with earlier statistical results. A sudden and dramatic change of this pattern was observed with the start of the storm main phase. During the main phase, wave amplitudes were greatly enhanced and the active wave region moved to considerably lower latitudes to the late evening MLT sector. Also, the existence of heavy ions in the later main phase changed the distribution of wave frequencies dramatically. Most interestingly, a number of oxygen band EMIC waves were observed during a limited period of about 7 hours in the later main phase. The observed asymmetric MLT distribution of these oxygen band waves implies that the oxygen loss rate is faster than the drift rate. The results suggest that the EMIC waves play a crucial role in the main and early recovery phase of a great storm.

1. Introduction

Electromagnetic ion cyclotron (EMIC) waves can be generated in the equatorial magnetosphere by anisotropic populations of energetic ions in an ion cyclotron instability [*Cornwall*, 1965; *Kennel and Petschek*, 1966]. The presence of both cold and energetic heavy ions (mainly He^+ and O^+) is known to have a remarkable effect to the amplification, spectra, and propagation of EMIC waves [see, e.g., *Young et al.*, 1981; *Fraser and McPherron*, 1982; *Gomberoff and Cuperman*, 1982; *Rauch and Roux*, 1982]. Increasing the concentration of a certain heavy ion species, wave generation is enhanced below and slightly suppressed above the respective gyrofrequency [*Gomberoff and Neira*, 1983; *Kozyra et al.*, 1984]. When propagating toward regions of a stronger magnetic field, the waves generated above the heavy ion gyrofrequency eventually meet a crossover frequency where polarization is changed. In a region where wave frequency and the local bi-ion hybrid frequency match, part of the wave is reflected. The amount of reflection increases with increasing heavy ion concentration. On the other hand, waves generated below the heavy ion gyrofrequency can freely propagate to lower altitudes in the left-handed (LH) mode [*Young et al.*, 1981]. The conducting ionosphere can reflect part of the incoming wave back to the magnetosphere. It can also couple part of the wave to a compressional mode which can be ducted in the ionospheric waveguide away from the foot point of the field line along which the wave was propagating [*Tepley and Landshoff*, 1966; *Manchester*, 1966, 1968; *Greifinger and Greifinger*, 1968]. On the ground, the EMIC waves are observed as Pc1 (or sometimes Pc2) type pulsations in the frequency range 0.2-5.0 Hz (0.1-0.2 Hz).

Ground-based studies have indicated a relation between geomagnetic activity and Pc1 pulsations. Structured (pearl-type) Pc1 activity tends to start 3-7 days after the main phase of the storm [*Wentworth*, 1964]. *Heacock and Kivinen* [1972] observed that structured Pc1 pulsations occur during the storm recovery phase, while unstructured Pc1 and Pc2 activity tends to prefer the initial and early recovery phase of storm. *Heacock and Akasofu* [1973] noted that structured Pc1 pulsations

Paper number 97JA02820.
0148-0227/97/98JA-02820$09.00

tend to occur at lower latitudes and with higher frequencies after severe magnetic storms, indicating that the location of the plasmapause, the preferred source region of structured Pc1 pulsations, depends on the intensity of the storm. They related the time delay between *Dst* minimum and the appearance of structured pulsations to the plasmasphere refilling rate and to the time needed to bring the ring current into the stable trapping limit.

Satellite studies of storm time occurrence and characteristics of Pc1 pulsations are few. *Anderson and Hamilton* [1993] found a strong correlation between magnetospheric compressions and onsets or enhancements of EMIC waves observed by AMPTE/CCE. *Erlandson et al.* [1994] made ground and satellite observations of a Pc1 event which was connected with enhanced magnetospheric compression during the recovery phase of a storm. They concluded that magnetospheric compressions can easily result in enhanced Pc1 pulsation activity during the recovery phase because of the additional energetic ions present in the magnetosphere after the storm. *Olson and Lee* [1983] studied theoretically the connection between magnetospheric compressions and Pc1 wave generation. During an adiabatic compression, particles gain preferably perpendicular energy leading to enhanced particle anisotropy and wave growth [*Kokubun*, 1970].

Development of the storm time ring current is determined by the trapped energetic particles injected into the inner magnetosphere during the storm main phase. The relative importance of different ring current loss mechanisms acting during the storm recovery phase was recently studied by *Fok et al.* [1996] and *Kozyra et al.* [1997]. Fok et al. concluded that pitch angle diffusion due to interaction with ion cyclotron waves [*Cornwall et al.*, 1970; *Williams and Lyons*, 1974] is needed in order to explain certain features of observed pitch angle distributions, especially in the high energy >100 keV range of ions.

In this paper we present EMIC wave observations made by the F1 double probe electric field instrument of the Swedish/German Freja satellite during the April 1993 storm. Almost continuous overview mode operation of the F1 instrument allowed us to follow the global wave activity during the whole storm period in April 2-8, 1993. In the next section we will present the instrumentation used in this study. In section 3 the Freja observations are presented and analyzed. In section 4 we will discuss the main results obtained in different phases of the storm. Finally, section 5 contains our summary.

2. Instrumentation

The Freja satellite [*Lundin et al.*, 1994] was launched on October 6, 1992, into a 63° inclination orbit with an orbital period of 109 min and apogee and perigee heights of 1750 and 600 km, respectively. Freja was spinning with a spin rate of 10 rpm and the spin axis was pointing toward the Sun within 30°. The apogee of the orbit was above the northern hemisphere and drifted around the Earth in about 100 days.

The F1 electric field instrument of Freja was a spherical double-probe instrument with three pairs of probe booms, all in the satellite spin plane [*Marklund et al.*, 1994]. F1 measured two components of the electric field from the voltage difference between the boom pairs. The output from the F1-instrument used here are the two orthogonal components of the electric field in the spin plane, E1 and E2. E1 is along the projection of magnetic field in the spin plane, and E2 is perpendicular to it.

In this study we use the so called overview mode measurements of F1. The instrument was operated in this mode continuously for up to 14 hours (about eight consecutive orbits) by storing the data in a 2 Mb onboard memory. In this mode, F1 makes electric field measurements at the rate of 8 samples/s, adequate to study ion cyclotron waves in the Pc1 frequency range. In addition, three Finnish search coil magnetometers were used to follow the ground Pc1 activity during the storm period. These stations are Sodankylä (SOD, 67.4° GGLat, 26.5° GGLong, $L = 5.1$), Oulu (OUL, 65.0° GGLat, 25.5° GGLong, $L = 4.3$), and Nurmijärvi (NUR, 60.5° GGLat, 24.7 ° GGLong, $L = 3.3$). The MLT of these stations is approximately MLT=UT+2.5 hours.

3. Observations

Nearly continuous F1 overview mode data were available from April 2, 1622 UT to April 8, 1711 UT (Freja orbits 2357-2436), covering the initial, main and recovery phases of the storm. The *Dst* index for this period is depicted in Figure 1a. During two days of initial compression the *Dst* index was fluctuating but reached finally about +20 nT. The storm sudden commencement (SSC) occurred at 1434 UT on April 4. The main phase started soon thereafter as depicted by the rapid descent of the Dst-index since 1600 UT. A local minimum of -108 nT was reached at 1900 UT, and a brief recovery phase followed thereafter, raising *Dst* up to -82 nT. However, another strong, but less rapid intensification continued the storm main phase, and on April 5 at 0700 UT the *Dst* index had reached its absolute minimum value of -169 nT. *Kp* index, which measures the global disturbance level, reached the maximum value of 8- at 2100-2400 UT on April 4. Later, the storm recovery was interrupted by additional moderate ring current enhancements, the two strongest occurring on April 6 and 8.

During these days the apogee of the Freja orbit was in the postnoon sector (1400-1500 MLT). In Figure 2 we have presented the Freja orbits for one full day (April 4) in a polar plot with circles and sectors representing the corrected geomagnetic latitudes (CGMLat) and MLT sectors, respectively. Northern (apogee) passes

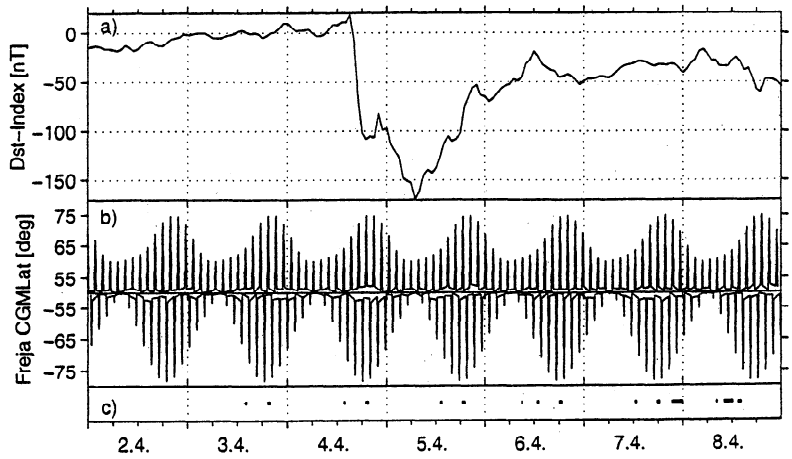

Figure 1. (a) *Dst* index of the storm period from April 2 to 8. (b) The development of Freja orbit from April 2 to 8. The part of the orbit with absolute CGM latitude exceeding 45° is shown only. (c) Times of missing overview mode data.

are presented with continuous and southern (perigee) passes with dotted lines. Only the high-latitude parts of the orbits exceeding 45° (absolute; unless otherwise mentioned, both northern and southern hemispheres are included) CGMLat are shown, each lasting about 20-30 min. The highest northern and southern CGM latitudes of each Freja orbit during April 2-8 are presented in Figure 1b. The regular diurnal variation of the magnetic latitude of subsequent apogees and perigees (caused by the tilt of the Earth's magnetic dipole) is clearly visible. During the present observations, the lowest apogee/perigee latitudes of about 60°/50° occurred during the morning hours, the highest latitudes of about 75°/78° in the evenings.

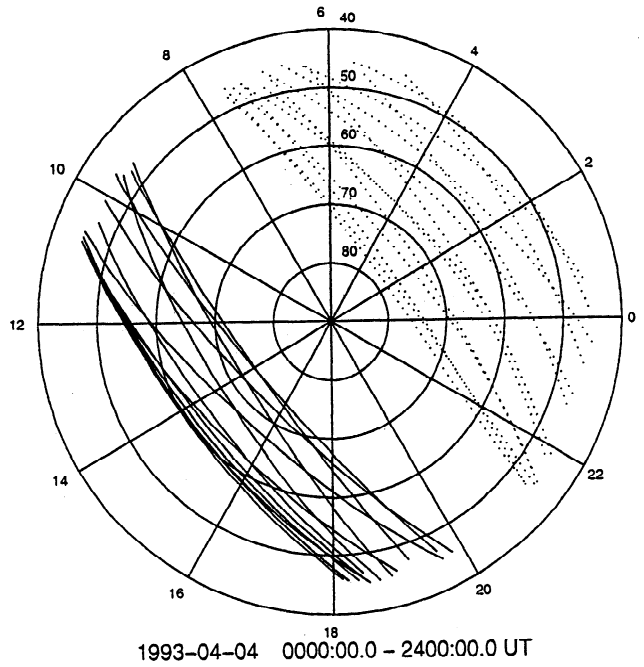

Figure 2. All 14 Freja orbits on April 4, 1993, as seen in MLT-CGMLat plane. Only the parts of orbit exceeding 45° CGMLat are shown. The northern (southern) passes are marked with solid (dashed) lines.

The overview mode measurements were nearly continuous, with only few apogee passes missing. The time intervals of missing data are marked in Figure 1c with short horizontal lines. In total, 49 Pc1 wave bursts were identified in F1 during the observed time. The first event occurred on April 2 at 1749 UT and the last one on April 8 at 1527 UT. All the Pc1 events were required to have a fairly regular waveform and a band limited spectral maximum in the Pc1 range (0.2 - 4 Hz) below the equatorial proton gyrofrequency F_{H+}. (The latter was calculated using the Tsyganenko, 1987, magnetic field model [*Tsyganenko*, 1987].) Almost all events had a stronger spectral maximum in the component perpendicular to the magnetic field, which is in accordance with the idea that the waves are mainly transverse polarized. These spectral features strongly suggest that the selected Pc1 events are indeed equatorial ion cyclotron waves. Event durations varied between 3 and 70 s, with a median (average) at 10 (respectively, 15) s. These durations are in good agreement with earlier EMIC wave observations made by Freja [*Mursula et al.*, 1994], Magsat [*Iyemori and Hayashi*, 1989], and DE 2 satellites [*Erlandson and Anderson*, 1996].

3.1. Sample Events

3.1.1. Event A. The sample event A (Plate 1) occurred in the very beginning of the storm main phase on April 4 at about 1610 UT. *Dst* index was -8 nT and had just started its rapid descent. *Kp* index was already as high as 6 during this event. Event A occurred in the late evening sector at about 2130 MLT and at a rather low southern latitude between -54° and -55° CGMLat.

Event A consists of two clearly separate strong bursts which were also treated as separate events in the statistical analysis to be discussed later. The first burst starts at 1609:28 UT and lasts about 15-20 s. With a

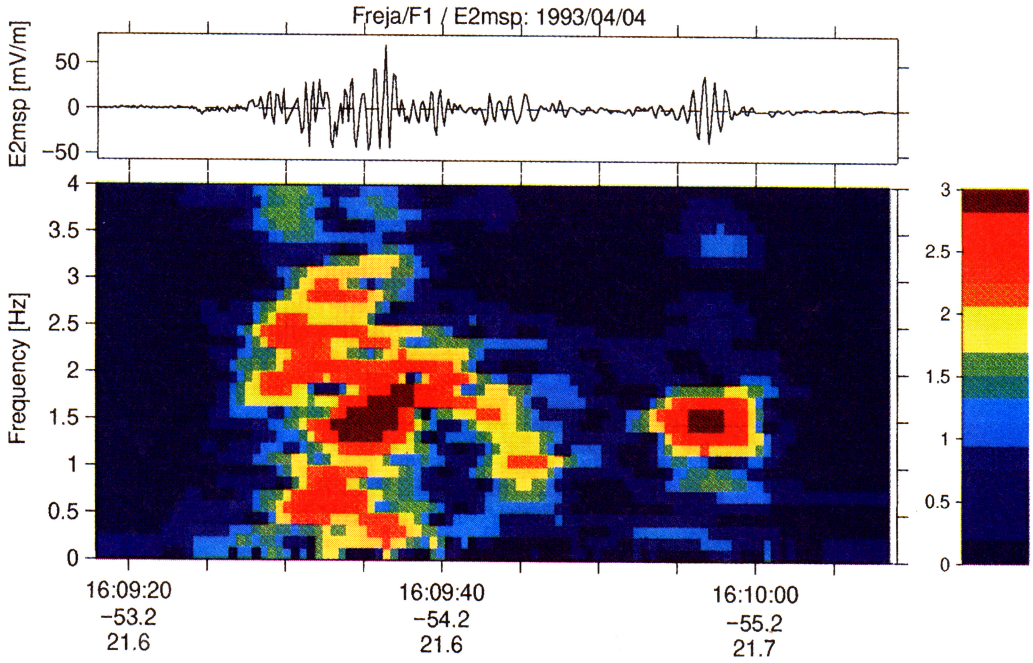

Plate 1. Sample event A. (top) The waveform and (bottom) the color-scaled dynamic spectrum of the E2 component of the event. Parameters below the bottom panel are UT time, CGM latitude (in degrees), and MLT time (in hours).

maximum amplitude of 54 mV/m in the E2 component it is the most powerful Pc1 burst observed during the whole storm. The spectral power maximum is between 1.1 and 2.2 Hz, i.e. clearly below the equatorial He^+ gyrofrequency F_{He+} (4.5 Hz) but slightly above F_{O+} (1.1 Hz). Also, there is evidence for a weaker maximum below F_{O+} and a spectral slot matching well with the calculated O^+-stop band. (There is a weak sub-burst of the first burst at 1609:42 UT with two spectral maxima, the latter close to the slot frequency. However this frequency is probably not stable and it is not e.g. seen in the E1 component (not shown) which has a single maximum at about 1.5 Hz).

The second burst of this event starts at 1609:53 and lasts about 7 s. The wave amplitude is again rather high, about 35 mV/m in the E2 component. The spec-

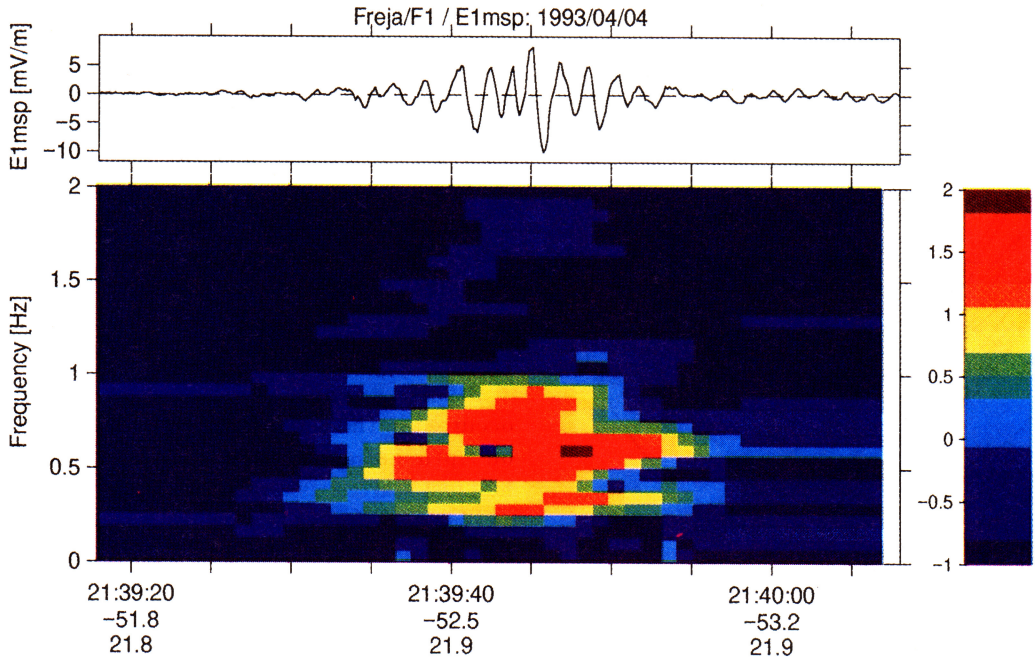

Plate 2. Same as Plate 1 for E1 component of sample event B.

tral power of this event is very clearly restricted between 1.1 and 1.7 Hz, i.e., to a slightly lower frequency range than the first burst. Since, because of the slightly higher latitude of the second burst, the equatorial heavy ion gyrofrequencies are also somewhat lower (F_{He^+} = 3.5 Hz, F_{O^+} = 0.9 Hz), and the observed frequency range of the second wave burst corresponds to the same equatorial wave growth band as in case of the first burst.

Note that the orbit of event A had a fairly high apogee latitude. Therefore the satellite was traversing latitudes fairly quickly, about 3° CGMLat/min at the time of event A. Accordingly, the (whole) first burst extended about 1° CGMLat. This is roughly twice that observed earlier in Freja during quiet geomagnetic times [*Mursula et al.*, 1994] and is probably due to the extraordinary strong signal and the very disturbed conditions. On the other hand, the second burst has a small latitude range of about 0.3° CGMLat only. Note also that the latitude range of the whole event A is as large as 1.6° CGMLat.

3.1.2. Event B. Event B (Plate 2) consists of one burst which occurred later during the main phase of the storm on April 4 at about 2140 UT and lasted about 20 s. The *Dst* index had a local minimum value of -106 nT, and the *Kp* index had its overall maximum of 8- during this event. Event B occurred also in the evening sector at about 2200 MLT and at a low southern latitude of about -53° CGMLat. Most interestingly, the spectral power of this event is confined between 0.4 and 0.7 Hz which is clearly below the equatorial O^+ gyrofrequency (1.1 Hz). In this event, the E1 component was slightly more intensive with an amplitude of about 8.8 mV/m. (The ratio between the E1 and E2 amplitudes depends on wave polarization. Since the angle between the spin plane normal and magnetic field direction was about 144° during this event, the wave may still have been mainly transverse polarized.) Note also that the waveform of event B (see Plate 2) is quite regular and shows evidence for dispersion, in good correspondence with a similar fully developed pearl observed earlier at Freja [*Mursula et al.*, 1994]. Also, the duration of the event is nearly the same as observed there. The latitude width of event B is about 0.6° CGMLat.

3.2. Spatial Distribution of Waves

Figure 3a shows the scatterplot of the (absolute values of) corrected geomagnetic latitudes of all events observed as a function of their time of occurrence, and Figure 3b shows their MLT times. The events detected in the northern hemisphere (close to apogee) are marked by crosses, and those in the southern hemisphere by open circles. The *Dst* index has been added in Figures 3a and 3b to allow comparison with the various phases of the storm. (Note that there is an event gap during the early morning hours in almost every day. This is due to the fact that the lowest apogee orbits occur at this time of the day during the period studied. See also Figure 1b).

As can be seen in Figure 3a, during the initial phase preceding the storm main phase (from April 2 to early April 4), waves are observed at geomagnetic latitudes from about 60° to as high as 72°. Except for one event, these events are found in the northern hemisphere from prenoon to evening MLT sector.

Several notable changes in the spatial distribution of waves occur when the main phase starts in the afternoon on April 4. With the decreasing *Dst* index during the main phase, waves are observed at lower and lower latitudes, even below 50°. (Note that this decrease is

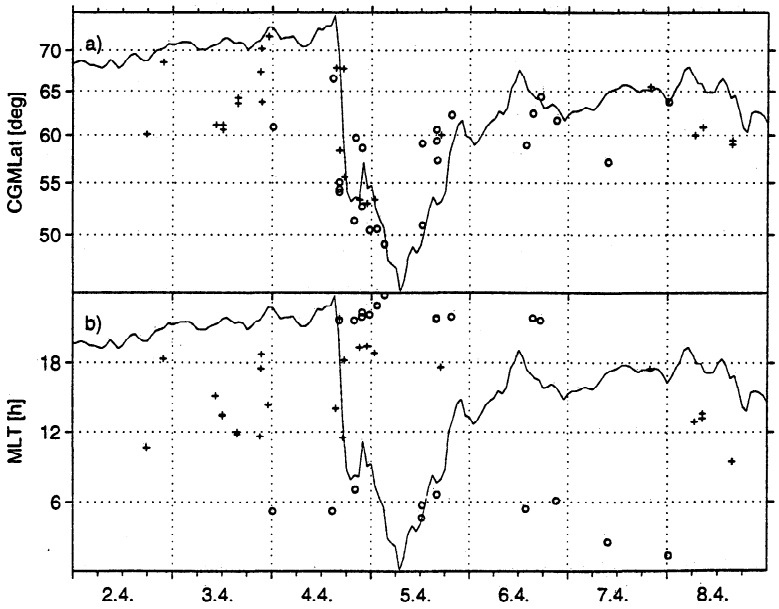

Figure 3. The scatterplot of (a) corrected geomagnetic latitudes and (b) MLT times of Pc1 events against UT. The northern latitudes are indicated by plus signs and the southern latitudes are indicated by open circles. The *Dst* index is also shown as a thin solid line.

not due to changes in Freja orbit since it starts already during orbits of increasing apogee (and perigee) latitude). Although the orbit varies similarly every day, no similar decrease is found on any other day studied. Moreover, the very low latitude waves are found only on sufficiently high latitude orbits, not on the very lowest latitude orbits. Except for three events in the early main phase, all waves during the main phase of the storm (from afternoon of April 4 to early April 5) were found at latitudes below 60°. Note also that no waves at the lowest latitudes (below) 55° CGMLat were found outside the main or early recovery phase of the storm.

The MLT distribution of waves observed during the storm main phase was also found to be dramatically different from that during the initial phase. The events during the main phase are found mainly in the late evening to premidnight (1800-2400 MLT) sector. This change in MLT is partly due to the decreasing latitude of events in the present orbit configuration. However, the evening preference of waves during main phase is clear since only four events were found in the morning-noon sector which is symmetric with the evening-midnight sector with respect to the orbit. We emphasize that despite the same diurnal orbital evolution of orbits every day, no similar low latitude/nightside population was observed during the several days studied here. (Note that the lowest *Dst* time occurs in the morning at the time of lowest-latitude Freja orbits. This limits our capability to observe waves in the relevant CGMLat/MLT sector. In particular waves above 55 ° CGMLat are out of reach at this time. However, since no events are observed on those orbits, we can still conclude that, even during the *Dst* minimum time, waves were not present at latitudes much lower that about 50° CGMLat).

As mentioned above, the lowest-latitude events disappear after the early recovery phase. Instead, during the storm recovery phase (from noon of April 5 onward), waves are observed between 57° and 66° CGMLat. It is interesting to note that this latitude distribution is several degrees lower than during the initial phase. Moreover, contrary to the initial phase, waves during most of the recovery phase occur mainly around midnight (early morning and late evening) rather than at similar latitudes around noon. Only on the last day studied (April 8) the MLT distribution is centered around noon, resembling the MLT distribution before the storm main phase.

3.3 Amplitude Characteristics

Figure 4a shows the amplitudes of the E2 components of observed wave events as a function of the time of their occurrence. Note that the amplitude axis is logarithmic. The event amplitude was defined to be one half of the highest peak-to-peak value during the event. (However, possible sporadic peaks occurring in some events were neglected.) An effective lower limit on the amplitude for the wave to be observed was about 0.5 mV/m. (The background was mainly due to residuals of the spin rate. These residuals remain in the data even after removing the induced electric field if the satellite ephemerides are known with insufficient accuracy. On the other hand, the minimum field observable by F1 was about 0.03 mV/m.) Both of the two electric field components (E1 and E2) were examined for all wave events. However, almost all events (46 of 49) had a larger amplitude in the E2 component.

As seen in Figure 4a most waves had amplitudes between 1 and 10 mV/m. The median value of the amplitude over the whole storm period was 4.8 mV/m. This is somewhat larger than found in earlier Freja observations during quiet geomagnetic conditions [*Mursula et al.*, 1994]. The three most intensive waves with amplitudes of several tens of mV/m were observed during the first 2 hours of the main phase of the storm (1600-1730 UT). All of them were found at very low geomagnetic latitudes below 56° CGMLat in the evening-premidnight sector. (Two of these highest amplitude bursts are seen in Plate 1, event A.) It is interesting to note that all the nine most intensive events with amplitudes larger than 10 mV/m occur during a period of decreasing *Dst* index. This is true for the five intensive events observed in the early main phase. It is also true for one strong event found at the start of the additional decrease of *Dst* index late on April 4, for another event in the early-recovery phase on April 5, and for two events occurring very late in the recovery phase on April 8. (Actually, the two last events occur during the main phase of a separate minor storm.)

3.4. Frequency Characteristics

The central frequencies of all the events are plotted in Figure 4b. The frequencies range from about 0.2 (which was the low-frequency limit imposed on the event selection) up to 3.1 Hz. The median frequency of the whole sample was 1.0 Hz, and roughly 60% of events were in the frequency range of 0.5-1.5 Hz. The overall frequency distribution corresponds fairly well to that observed earlier but based on a smaller number of events [*Mursula et al.*, 1994]. Note also that waves had a significantly lower average frequency in the initial phase than in the recovery phase of the storm. This corresponds to the observed difference of average latitude of events during these two times (see Figure 3a). If other parameters are constant, higher frequencies are expected at lower latitudes, corresponding to the higher value of the equatorial magnetic field.

The event frequencies normalized by the corresponding (calculated) equatorial He^+ gyrofrequency are presented in Figure 4c. The equatorial H^+, He^+, and O^+ gyrofrequencies are indicated by a dashed-dotted, solid and dashed lines, respectively. About 70% of the events were found with a frequency below the corresponding He^+ gyrofrequency (normalized frequency < 1). This

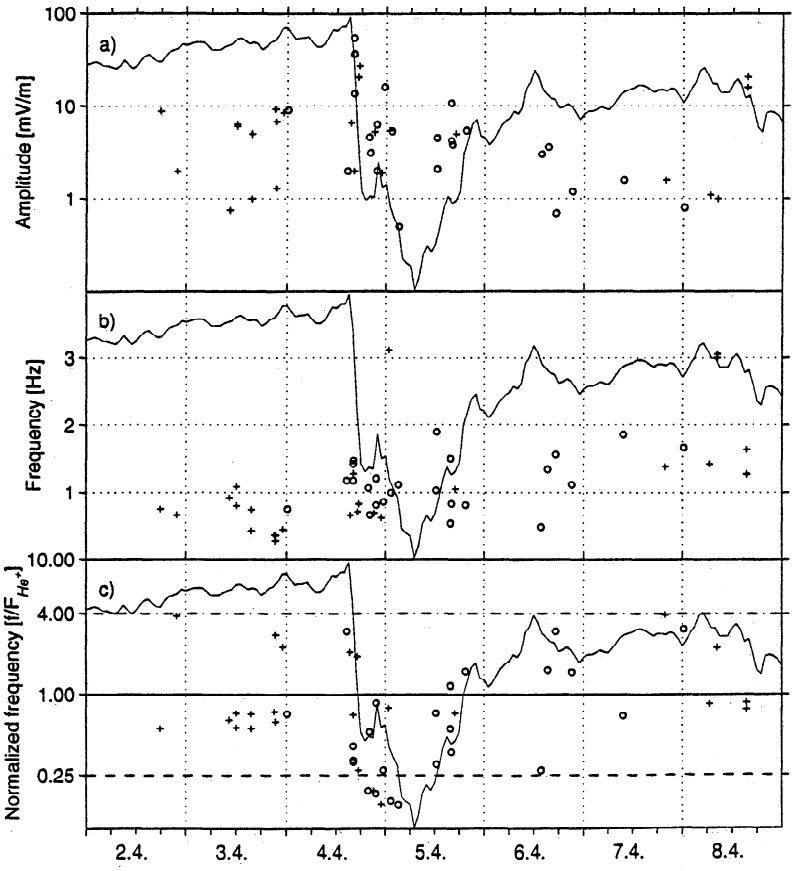

Figure 4. The scatterplot of (a) amplitudes, (b) frequencies, and (c) normalized frequencies of all Pc1 events against UT. In bottom panel equatorial H^+, He^+ and O^+ gyrofrequencies are indicated by dashed-dotted, solid, and dashed lines, respectively.

clearly shows the significance of heavy ions (in particular He^+ ions) on wave growth during the period studied. Events with normalized frequency larger than 1 were found during all other phases of the storm except for late main phase and early recovery phase. Instead, during late main and early recovery phase, all events had a normalized frequency below 1, and several events were found whose frequency was below the corresponding equatorial O^+ frequency. Note that these were the only oxygen band events found during the whole 7-day period studied. (The calculation of equatorial gyrofrequencies may be somewhat uncertain especially during the storm main phase even at low latitudes. Uncertainties in the satellite's magnetic location may also cause some errors in these calculations. However, taking into account the number of events and the range of their normalized frequencies, there is no doubt that oxygen band waves have been observed.)

3.5. Ground Observations

Recordings of three Finnish search-coil magnetometer stations were used to follow the pulsation activity on ground during the storm. There was weak Pc1 activity at all stations on April 2 - 3. On April 4, during enhanced compression (as evidenced by a positive *Dst* index) at 0730-1300 UT, strong Pc1 pulsations were observed at SOD, and weaker at OUL and NUR. At about 1500 UT on April 4, simultaneously with the storm main phase, a long interval of PiC and PiB type activity started, consisting of several separate intensifications and lasting for most of the evening and the following day. No significant Pc1 waves were observed at any station from the start of the main phase until late recovery phase. Pc1 pulsation activity started again on April 7 and was intensified on April 8. This verifies the pattern of occurrence of Pc1 waves on ground obtained from earlier storm studies [*Wentworth*, 1964] that Pc1's reappear on ground only several days after the storm main phase. The ground observations will be presented and analyzed in more detail in a separate paper.

4. Discussion

4.1. Compression Phase

During the initial (compression) phase the increasing solar wind pressure against the magnetosphere leads to an increase of proton anisotropy and thereby enhances Pc1 wave activity in the dayside outer magneto-

sphere [*Olson and Lee*, 1983]. The connection between compressions and increased Pc1 wave activity has been demonstrated using both ground based [e.g., *Heacock and Hessler*, 1965; *Hirasawa*, 1981] and satellite observations [*Anderson and Hamilton*, 1993; *Erlandson et al.*, 1994].

As a good example of this connection between compressions and Pc1 activity, Freja observed a wave event at 1433 UT on April 4, almost exactly at the time of the SSC which has been identified on ground at 1434 UT. This event occurred when Freja was at a high southern latitude (-66.7° CGMLat) in the morning sector (at about 0510 MLT). The frequency of the event (about 1.2 Hz) was higher than in all other events during the initial phase, although several events were found at lower latitudes. This also demonstrates the fact that significant compressions tend to increase the wave frequency [*Troitskaya et al.*, 1968; *Olson and Lee*, 1983; *Kangas et al.*, 1986].

Freja observed wave events during the initial phase in the geomagnetic latitudes from 60° to as high as 72°, clearly higher than during other phases of the storm. All but one event were observed in the prenoonside to eveningside (1000-1900 MLT) magnetosphere. This is in accordance with the afternoon, high-latitude maximum of Pc1 wave occurrence determined by the equatorial AMPTE/CCE observations [*Anderson et al.*, 1992]. (As noted above, the latitude and MLT distributions are slightly correlated by the orbit configuration. However, the dominance of afternoon/evening sector events over morning sector during the compression phase is evident in Figure 3b.)

4.2. Main and Early Recovery Phase

During the storm main phase, energetic particles are injected into the inner magnetosphere from the magnetospheric tail. These particles drift around the Earth on closed drift shells and form the storm time ring current. The storm time ring current can penetrate as deep as L = 2-3 depending on the intensity of the storm. During the minimum *Dst* phase (averaged over 20 storms) the relative number densities of particles in the energy range 30-315 keV at L = 3-5 were found to be 77% protons and 17% O^+ ions, while in the quiet time they were 96% protons and only 2% O^+ [*Gloeckler and Hamilton*, 1987]. These differences indicate strong variations in the magnetospheric ion content with geomagnetic activity. *Cladis and Francis* [1985] showed that all of the O^+ ions and most of the protons appearing in the ring current during the main phase originate from the polar regions of the ionosphere. *Hamilton et al.* [1988] studied the development of the ring current during the great February 1986 storm using CHEM particle instrument measurements onboard AMPTE/CCE. They noted that the great intensification of the ring current is caused by O^+ and N^+ ions and that the loss of these heavy ions is also the reason for the rapid initial recovery, which is a typical feature for great storms. During the February 1986 storm the energy density of O^+ ions exceeded that of protons in the inner ring current during the minimum *Dst*. The maximum of the radial distribution of the ring current energy density at that time was found at about L = 2.6.

The high-amplitude waves observed by Freja at low latitudes in the evening-midnight sector during the storm main phase are due to the enhanced amplification caused by new anisotropic energetic ions entering the inner magnetosphere. A large portion of these new particles is expected to be oxygen ions [*Gloeckler and Hamilton*, 1987]. This could account for the unusually low normalized frequencies of the waves during the later main phase, many of which are below the equatorial O^+ gyrofrequency (see Figure 4c). The existence of oxygen ions enhances the wave growth below the O^+ gyrofrequency relative to the two other bands (one between F_{O+} and F_{He+}, the other between F_{He+} and F_{H+}) [*Kozyra et al.*, 1984]. These oxygen band waves can fairly easily propagate to low altitudes since no heavier ions exist to form stop bands for their propagation from the equator to ground. On the other hand, waves produced in the other bands above the equatorial F_{O+} (or F_{He+}) would encounter the oxygen (helium) stop band and find it more difficult to propagate to the ionosphere. An enhanced amount of heavy ions can therefore explain the fact that all waves observed during the later main phase and early recovery phase (on several orbits around minimum *Dst*) were below the helium gyrofrequency (normalized frequency < 1; see Figure 4c).

Before the present study, only few studies have observed O^+ band EMIC waves in the magnetosphere. *Inhester et al.* [1984] found large-amplitude Pc2 waves in GEOS 2 data in connection with geomagnetic disturbances caused by several successive substorms. *Fraser et al.* [1992] observed EMIC waves around F_{O+} using ISEE 1 and 2 spacecraft in the plasmapause/plasmatrough region in the late afternoon sector close to the equator. Events were observed after strong substorm activity, when the density of warm O^+ and He^+ ions was enhanced in outer plasmasphere, leading to a local minimum of Alfvén velocity and thereby enhancing amplification of EMIC waves. These studies verify the view that only during strong magnetospheric perturbations (substorm/storm activity) a sufficient amount of O^+ ions is extracted from the ionosphere into the magnetosphere in order for O^+ band EMIC waves to be generated. All these studies observed O^+ waves close to their equatorial generation region. Therefore the present study shows that the O^+ band EMIC waves can indeed propagate from the equator down to ionospheric altitudes. Similar O^+ band waves at ionospheric altitudes were recently observed by *Erlandson and Anderson* [1996].

As already mentioned, the highest amplitude events were observed in the very early main phase. It is inter-

esting to note that these waves were not oxygen but helium band waves. It is probable that in the very early main phase, the wave growth was already greatly enhanced at the equator due to the new energetic protons, but the number of oxygen ions was still too small to seriously affect wave growth at the equator or wave propagation from the equator to the ionosphere. However, only a couple of hours later, still during the storm main phase, wave amplitudes observed at ionospheric heights were considerably lower, oxygen band waves had appeared, and waves above helium gyrofrequency had disappeared. This implies that the timescale of forming the oxygen ring current is only couple of hours.

As depicted in Figure 3a, the latitude distribution of EMIC waves observed by Freja changes dramatically soon after the start of the storm main phase. While all events in the initial phase were located above 60° CGMLat, all events during the later main and early recovery phase were below this latitude. In particular, all the oxygen events were restricted between 49°-54° CGMLat, i.e., $L = 2.3$-2.8. This agrees remarkably well with the maximum energy density position at $L = 2.6$ determined for the February 1986 storm [*Hamilton et al.*, 1986]. Accordingly, EMIC waves seem to follow closely the movement of the energy density maximum of the ring current to lower L shells.

It is also expected that together with increasing activity, the position of plasmapause moves to lower L shells. Since the plasma density affects EMIC wave generation and the plasmapause forms appropriate conditions for wave propagation to lower altitudes [*Mazur and Potapov*, 1983], the movement of the plasmapause may be partly responsible for the appearance of waves at lower L shells. The fact that all O^+ band waves were found at very low latitudes is also in accordance with the result that their amplification is largest inside the plasmapause [*Hu and Fraser*, 1994]. However, neither the extension of the ring current or the plasmapause motion can explain the complete absence of waves above 60° CGMLat around minimum Dst period. This may partly be due to the stop bands formed by the large amount of heavy ions flowing out of the polar ionosphere [*Cladis and Francis*, 1985], or complete quenching of waves by resonant absorption as recently suggested by *Thorne and Horne* [1997]. Another explanation may be that since auroral activity also moves to lower L shells during the storm main phase, the band limited EMIC waves can not be observed among increased turbulence on these field lines. (A similar problem was noted by *Erlandson and Anderson* [1996].)

As seen in Figure 4c, the oxygen band waves are only observed for about 7 hours. (Unfortunately, the existence of three subsequent very low-latitude orbits decreases the wave observability after the detection of the last oxygen band wave, and thus the above estimate may be roughly twice longer.) Assuming that the oxygen ion energies are of the same order of magnitude (about 100 keV) as observed by *Gloeckler and Hamilton* [1987], their drift times should be approximately 2-4 hours. Accordingly, since oxygen band waves were found during a longer time, one would expect to find them at different MLT sectors. However, all the oxygen waves were found in the evening-midnight sector and, in particular, none were observed in the prenoon sector, which is in a symmetrical position with respect to the orbit. This implies a very asymmetric ring current during the main phase and suggests that the oxygen ion loss rate is considerably faster than the drift speed. These results are difficult to explain in terms of the conventional ring current loss mechanisms (charge exchange and Coulomb scattering) and suggest that the production of EMIC waves contributes significantly to ring current decay during the main and early recovery phase. *Kozyra et al.* [1997] made ion convection model simulations including the charge exchange and Coulomb collisions as well as wave particle interactions as processes to scatter particles into the loss cone. They suggest that strong EMIC waves produced in the main and early recovery phase could partially account for the rapid decrease of the ring current in the early recovery of a storm. The present observations strongly support this interpretation.

4.3. Later Recovery Phase

The different energy and pitch angle dependences in charge exchange, Coulomb collision and drift for the three main ions (H^+, He^+, and O^+) cause these particle species to behave differently in the course of recovery. When simulating the time evolution of the distribution function during the recovery phase, *Jordanova et al.* [1996] noted that the particle distribution in the later recovery favours the generation of Pc1 pulsations in the morning MLT sector. Indeed, the later recovery phase is known to be the preferred time of occurrence of structured Pc1 pulsations on the ground [e.g., *Saito*, 1969]. Freja observations verify that there is persistent EMIC wave activity in the morning sector (see Figure 3b) throughout the recovery phase (April 5-7). The wave activity is slowly decreasing during this time, as demonstrated clearly by the very regular decrease of wave amplitude during April 5-7 (see Figure 4a). (This continues until the main phase of another minor storm increases wave amplitudes on April 8.) This decrease corresponds well to the decrease of the ring current during the later recovery phase. Although the intensity decrease is expected to be global, it is interesting to note that no waves are seen in the evening sector after April 6, while the morning sector still remain active (Figure 3b). This agrees well with the above mentioned calculation by *Jordanova et al.* [1996] and the ground-based results from much earlier years.

The latitude of waves observed by Freja increases rather rapidly to about 60° CGMLat soon after the minimum Dst time, and remains nearly constant during the whole subsequent recovery phase. (However, there

is some indication for a slow increase of latitude during the recovery phase (see Figure 3a)). Accordingly, the average latitude of EMIC waves remains some 4°-5° CGMLat lower during the whole recovery phase than observed in the initial phase. This reflects the fact that the ring current extends to lower L shells than initially, still long after the main phase. The near constancy of the latitude reflects the slow decay of the ring current during the later recovery phase.

Note also that the plasmasphere is expected to shrink during the storm main phase and expand again during the recovery phase. Thus both the plasmasphere and ring current evolution may contribute to the observed time evolution of the spatial (latitude, MLT) distribution of waves. It is also interesting to note that the average wave frequency is considerably higher in the recovery phase than in the initial phase (see Figure 4b). This is mainly due to the lower latitude of waves in the recovery phase as discussed above (see Figure 3a). Note also that a larger fraction of waves seems to have a frequency above F_{He+} (normalized frequency > 1) in the later recovery phase than in the initial phase of the storm, partly contributing to the observed higher average frequency in the recovery phase.

5. Summary

Freja satellite and its double probe electric field instrument have been found to be valuable tools in Pc1 wave studies. Here we have studied the occurrence and properties of Pc1 waves over a full geomagnetic storm from April 2 to 8, 1993. During the initial phase of the storm the waves are found in the high-latitude dayside magnetosphere and seem to be induced by magnetospheric compression, in good agreement with the earlier statistical studies of Pc1 wave occurrence [*Anderson et al.*, 1992; *Anderson and Hamilton*, 1993]. A sudden and dramatic change of this pattern was observed with the start of the storm main phase. In the beginning of the main phase the wave amplitudes were enhanced by one order of magnitude. During the main phase the active wave region moved to considerably lower latitudes to the late evening MLT sector.

Moreover, the distribution of wave frequencies changed radically during the main phase due to the effect of heavy ions. In particular, a number of oxygen band EMIC (ion cyclotron) waves were identified for about 7 hours in the later main phase. Using the observed asymmetric MLT distribution of these oxygen band waves, we argued that the oxygen ion loss rate is faster than the drift rate. The results suggest that the EMIC waves play an important role in the main and early recovery phase [*Kozyra et al.*, 1997], being probably the dominant factor in the loss of oxygen ions and, hence responsible for the rapid initial recovery of a great storm. In the later recovery phase the waves followed the slow decay of the ring current at a nearly constant L shell. The most persistent wave activity was found in the morning sector, in agreement with earlier ground based observations and recent simulations [*Jordanova et al.*, 1996].

The results depict the usefulness of EMIC waves as a method of following and diagnosting the state and evolution of the inner magnetosphere, in particular, the ring current and plasmapause. Although the many new features presented in this paper are conclusive, they are based on one single great storm and need to be confirmed by additional storm studies.

Acknowledgments. The computational assistance by Reijo Rasinkangas is greatly appreciated. This work has been financially supported by the Finnish Academy.

The editor thanks Brian J. Fraser and Robert Erlandson for their assistance in evaluating this paper.

References

Anderson, B. J., and D. C. Hamilton, Electromagnetic ion cyclotron waves stimulated by modest magnetospheric compressions, *J. Geophys. Res., 98*, 11369-11382, 1993.

Anderson, B. J., R. E. Erlandson, and L. J. Zanetti, A statistical study of Pc 1 - 2 magnetic pulsations in the equatorial magnetosphere, 1, Equatorial occurrence distributions, *J. Geophys. Res., 97*, 3075-3088, 1992.

Cladis, J. B., and W. E. Francis, The polar ionosphere as a source of the storm time ring current, *J. Geophys. Res., 90*, 3465-3473, 1985.

Cornwall, J. M., Cyclotron instabilities and electromagnetic emission in the ultra low frequency and very low frequency ranges, *J. Geophys. Res., 70*, 61-69, 1965.

Cornwall, J. M., F. V. Coroniti, and R. M. Thorne, Turbulent loss of ring current protons, *J. Geophys. Res., 75*, 7699-7709, 1970.

Erlandson, R. E., and B. J. Anderson, Pc 1 waves in the ionosphere: A statistical study, *J. Geophys. Res., 101*, 7843-7857, 1996.

Erlandson, R. E., L. J. Zanetti, M. J. Engebretson, R. Arnoldy, T. Bösinger, and K. Mursula, Pc 1 waves generated by a magnetospheric compression during the recovery phase of a geomagnetic storm in *Solar Wind Sources of Magnetospheric Ultra-Low-Frequency Waves, Geophys. Monogr. Ser.*, vol. 81, edited by M. J. Engebretson, K. Takahashi, and M. Schuler, pp. 399-407, AGU, Washington, D. C., 1994.

Fok, M.-C., T. E. Moore, and M. E. Greenspan, Ring current development during storm main phase, *J. Geophys. Res., 101*, 15311-15322, 1996.

Fraser, B. J., and R. L. McPherron, Pc1-2 magnetic pulsation spectra and heavy ion effects at sychronous orbit: ATS 6 results, *J. Geophys. Res., 87*, 4560-4566, 1982.

Fraser, B. J., J. C. Samson, Y. D. Hu, R. L. McPherron, and C. T. Russell, Electromagnetic ion cyclotron waves observed near the oxygen cyclotron frequency by ISEE 1 and 2. *J. Geophys. Res., 97*, 3063-3074, 1992.

Gomberoff, L., and S. Cuperman, Combined effect of cold H^+ and He^+ ions in the proton cyclotron electromagnetic instability, *J. Geophys. Res., 87*, 95-100, 1982.

Gomberoff, L., and R. Neira, Convective growth rate of ion cyclotron waves in a H^+-He^+ and H^+-He^+-O^+ plasma, *J. Geophys. Res., 88*, 2170-2174, 1983.

Gloeckler, G., and D. C. Hamilton, AMPTE ion composition results, *Phys. Scr., T18*, 73-84, 1987.

Greifinger, C., and P. S. Greifinger, Theory of hydromagnetic propagation in the ionospheric waveguide, *J. Geophys. Res., 73*, 7473-7490, 1968.

Hamilton, D. C., G. Gloeckler, F. M. Ipavich, W.

Stüdemann, B. Wilken, and G. Kremser, Ring current development during the great geomagnetic storm of February 1986, *J. Geophys. Res., 93*, 14343-14355, 1988.

Heacock, R. R., and S.-I. Akasofu, Periodically structured Pc1 micropulsations during the recovery phase of intense magnetic storms, *J. Geophys. Res., 78*, 5524-5536, 1973.

Heacock, R. R., and V. P. Hessler, Pearl-type micropulsations associated with magnetic storm sudden commencements, *J. Geophys. Res., 70*, 1103-1111, 1965.

Heacock, R. R., and M. Kivinen, Relation of Pc1 micropulsations to the ring current and geomagnetic storms, *J. Geophys. Res., 77*, 6746-6760, 1972.

Hirasawa, T., Effects of magnetospheric compression and expansion on spectral structure of ULF emission, *Mem. Natl. Inst. Polar Res. Jpn., 18*, 127, 1981.

Hu, Y. D., and B. J. Fraser, Electromagnetic ion cyclotron wave amplification and source regions in the magnetosphere, *J. Geophys. Res., 99*, 263-272, 1994.

Inhester, B., U. Wedeken, A. Korth, S. Perraut, and M. Stokholm, Ground-satellite coordinated study of the April 5, 1979 events: Observation of O^+ cyclotron waves, *J. Geophys., 55*, 134-141, 1984.

Iyemori, T., and K. Hayashi, Pc1 micropulsations observed by Magsat in the ionospheric *F* region, *J. Geophys. Res., 94*, 93-100, 1989.

Jordanova, V. K., L. M. Kistler, J. U. Kozyra, G. V. Khazanov, and A. F. Nagy, Collisional losses of ring current ions, *J. Geophys. Res., 101*, 111-126, 1996.

Kangas, J., A. Aikio, and J. V. Olson, Multistation correlation of ULF pulsation spectra associated with sudden impulses, *Planet. Space Sci., 34*, 543-553, 1986.

Kennel, C. F., and H. E. Petschek, Limit on stably trapped particle fluxes, *J. Geophys. Res., 71*, 1-27, 1966.

Kokubun, S., Fine structure of ULF emissions in the frequency range of 0.1-2 Hz, *Rep. Ionos. Space Res. Jpn., 24*, 24-44, 1970.

Kozyra, J. U., T. E. Cravens, A. F. Nagy, E. G. Fontheim, and R. S. B. Ong, Effects of energetic heavy ions on electromagnetic ion cyclotron wave generation in the plasmapause region, *J. Geophys. Res., 89*, 2217-2233, 1984.

Kozyra, J. U., V. K. Jordanova, R. B. Horne, and R. M. Thorne, Modeling of the contribution of electromagnetic ion cyclotron (EMIC) waves to stormtime ring current erosion, in *Magnetic Storms, Geophys. Monogr. Ser.*, vol. 98, edited by B. T. Tsurutani, W. D. Gonzalez, Y. Kamide, and J. K. Arballo, pp. 187-202, AGU, Washington, D. C., 1997.

Lundin, R., G. Hearendel, and S. Grahn, The Freja science mission, *Space Sci. Rev., 70*, 405-419, 1994.

Manchester, R. N., Propagation of Pc1 micropulsations from high to low latitudes, *J. Geophys. Res., 71*, 3749-3754, 1966.

Manchester, R. N., Correlation of Pc 1 micropulsations of spaced stations, *J. Geophys. Res., 73*, 3549-3556, 1968.

Marklund, G., L. G. Blomberg, P.-A. Lindqvist, C.-G. Fälthammar, G. Haerendel, F. Mozer, A. Pedersen, and P. Tanskanen, The double probe electric field experiment on Freja: Experiment description and first results, *Space Sci. Rev., 70*, 483-508, 1994.

Mazur, V. A., and A. S. Potapov, The evolution of pearls in the Earth's magnetosphere, *Planet. Space Sci., 31*, 859-863, 1983.

Mursula, K., L. G. Blomberg, P.-A. Lindqvist, G. T. Marklund, T. Bräysy, R. Rasinkangas, and P. Tanskanen, Dispersive Pc1 bursts observed by Freja, *Geophys. Res. Lett., 21*, 1851-1854, 1994.

Olson, J. V., and L. C. Lee, Pc1 wave generation by sudden impulses, *Planet. Space Sci., 31*, 295-302, 1983.

Rauch, J. L., and A. Roux, Ray tracing of ULF waves in a multicomponent magnetospheric plasma: Consequences for the generation mechanism of the ion cyclotron waves, *J. Geophys. Res., 87*, 8191-8198, 1982.

Saito, T., Geomagnetic pulsations, *Space Sci. Rev., 10*, 319-412, 1969.

Teplcy, L. R., and R. K. Landshoff, Wavequide theory for ionospheric propagation of hydromagnetic emissions, *J. Geophys. Res., 71*, 1499, 1966.

Thorne, R. M., and R. B. Horne, Modulation of electromagnetic ion cyclotron instability due to interaction with ring current O^+ during magnetic storms, *J. Geophys. Res., 102*, 14155-14163, 1997.

Troitskaya, V. A., E. T. Matveyeva, K. G. Ivanov, and A. V. Gulyelmi, Change in the frequency of Pc1 micropulsations during a sudden deformation of the magnetosphere, *Geomagn. Aeron., 8*, 784-786, 1968.

Tsyganenko, N. A., Global quantitative models of the geomagnetic field in the cislunar magnetosphere for different disturbance levels, *Planet. Space Sci., 35*, 1347-1358, 1987.

Wentworth, R. C., Enhancement of hydromagnetic emissions after geomagnetic storms, *J. Geophys. Res., 69*, 2291-2298, 1964.

Williams, D. J., and L. R. Lyons, The proton ring current and its interaction with the plasmapause: Storm recovery phase, *J. Geophys. Res., 79*, 4195-4207, 1974.

Young, D. T., S. Perraut, A. Roux, C. De Villedary, R. Gendrin, A. Korth, G. Kremser, and D. Jones, Wave-particle interactions near Ω_{He+} observed on GEOS 1 and 2, 1, Propagation of ion cyclotron waves in He^+-rich plasma, *J. Geophys. Res., 86*, 6755-6772, 1981.

T. Bräysy, K. Mursula, Department of Physical Sciences, University of Oulu, P.O.Box 333, FIN-90571 Oulu, Finland. (e-mail: timo.braysy@oulu.fi, kalevi.mursula@oulu.fi)

G. Marklund, Alfvén Laboratory, Royal Institute of Technology, S-10044 Stockholm, Sweden. (e-mail: marklund@plasma.kth.se)

(Received April 17, 1997; revised September 30, 1997; accepted October 3, 1997.)